

QCD phase diagram and charge fluctuations

K. Redlich^{a,b}, B. Friman^b and C. Sasaki^b

^a Institute of Theoretical Physics, University of Wrocław, PL-50204 Wrocław, Poland

^b Gesellschaft für Schwerionenforschung, GSI, D-64291 Darmstadt, Germany

Abstract. We discuss the phase structure and fluctuations of conserved charges in two flavor QCD. The importance of the density fluctuations to probe the existence of the critical end point is summarized. The role of these fluctuations to identify the first order phase transition in the presence of spinodal phase separation is also discussed.

1. Introduction

One of the essential predictions of QCD is the existence of a phase boundary in the (T, μ_q) -plane that separates the chirally broken hadronic phase from chirally symmetric quark-gluon plasma phase [1]. Arguments based on effective model calculations [1-12] indicate that at large μ_q the transition along this boundary line can be first order. In the opposite limit of high temperature and low baryon number density the transition from hadronic to quark gluon plasma phase is expected to be continuous or second order depending on the number of quark flavors and the quark masses [7-12]. This suggests that the QCD phase diagram can exhibit a critical endpoint where the line of first order phase transitions matches that of second order or analytical crossover [13]. The critical properties of this second order critical endpoint are expected to be determined by the Ising model universality class [5, 7, 12]. The existence of a critical end point in QCD has recently been studied in lattice calculations at non-vanishing chemical potential in 2- and (2+1)-flavor QCD [14, 15, 16].

In this paper we discuss how a generic QCD phase diagram appears in effective chiral model calculations. We consider the properties of the fluctuations of the conserved charges to identify the position of the phase boundary and the critical end point. We compare the model results with recent LGT findings in 2-flavor QCD and discuss their physical interpretation. Finally, considering deviations from an idealized equilibrium picture of the first order chiral phase transition we discuss the properties of charge density fluctuations by including spinodal instabilities.

2. Charge density fluctuations in effective chiral models and in LGT

To study thermodynamics and the phase structure related with the chiral symmetry in QCD we adopt the Nambu–Jona-Lasinio model formulated in the mean field

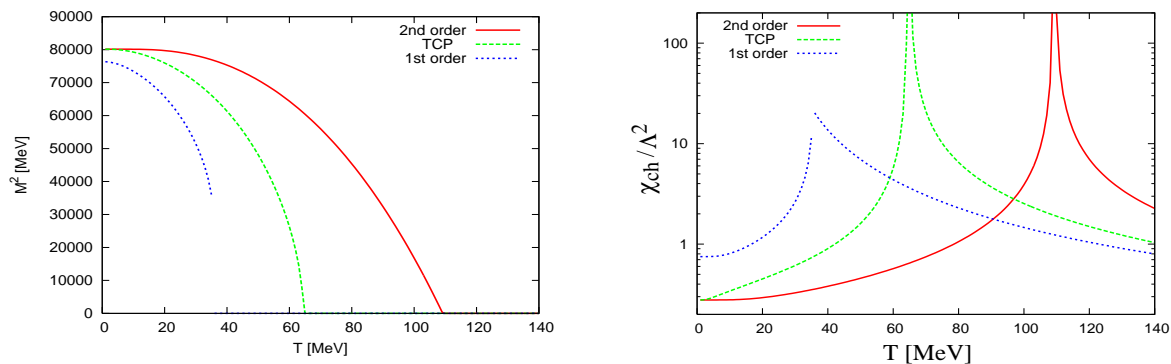


Figure 1. The chiral condensate M (left-hand figure) and the chiral susceptibility χ_{ch} (right-hand figure) calculated in the NJL model in the chiral limit as a function of temperature for different values of $\mu_q = 300, 275$ and 200 MeV corresponding to a 1st order, the tricritical point and a 2nd order transition [9].

approximation [6, 9]. In the chiral limit this model describes the chiral phase transition from a phase of massive quarks with dynamically generated mass $M(T, \mu_q)$ dependent on temperature T and quark chemical potential μ_q to a phase of massless quarks.

The effective quark mass $M(T, \mu_q)$ is a measure of the thermal expectation value of the quark condensate at finite T and μ_q . Thus, $M(T, \mu_q)$ acts as an order parameter for chiral symmetry restoration. In the chirally broken phase $M \neq 0$ and it vanishes when the symmetry is restored. In the Fig. 1-left we show the T -dependence of the dynamical quark mass for different values of μ_q . For small μ_q the condensate continuously melts in the narrow temperature range indicating the second order phase transition. At large μ_q the condensate M drops discontinuously from a finite to zero value indicating the first order nature of the chiral transition. The fluctuations of the order parameter $\chi_{ch} = \langle M^2 \rangle - \langle M \rangle^2$, shown in the Fig. 1-right, are finite when crossing the first order transition whereas they diverge at the second order line. The divergence is directly linked to the appearance of a massless mode in the scalar-isoscalar, so called sigma channel, if the transition is second order. The resulting phase diagram obtained in the NJL model with the particular set of the model parameters and in the chiral limit is shown in the Fig.2-left. It exhibits the generic, QCD-like structure discussed in the introduction. For a finite quark mass the second order transition is converted to a cross-over transition [1].

The existence of the tricritical point (TCP) is seen in Fig. 2-left to be strictly related with the strength of the four-fermion interactions in the isovector-vector channel controlled by the coupling G_V in the NJL Lagrangian. For large $G_V > 0.6G_S$ (with G_S describing the strength of the scalar four-fermion interactions) the TCP disappears from the phase diagram due to strong repulsive interactions in the medium.

The position of the TCP can be identified by considering the fluctuations of the charge density n_q that are quantified by the corresponding susceptibilities $\chi_q = \partial n_q / \partial \mu_q$

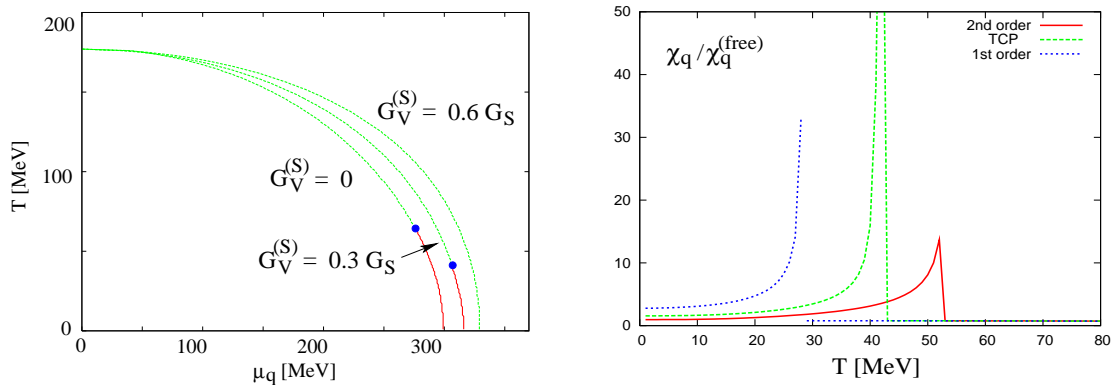


Figure 2. The left-hand figure: The NJL model phase diagram in the chiral limit for different values of the isovector-vector coupling G_V . The right-hand figure shows the net quark number fluctuations for $\mu_q = 310, 305$ and 300 MeV [9].

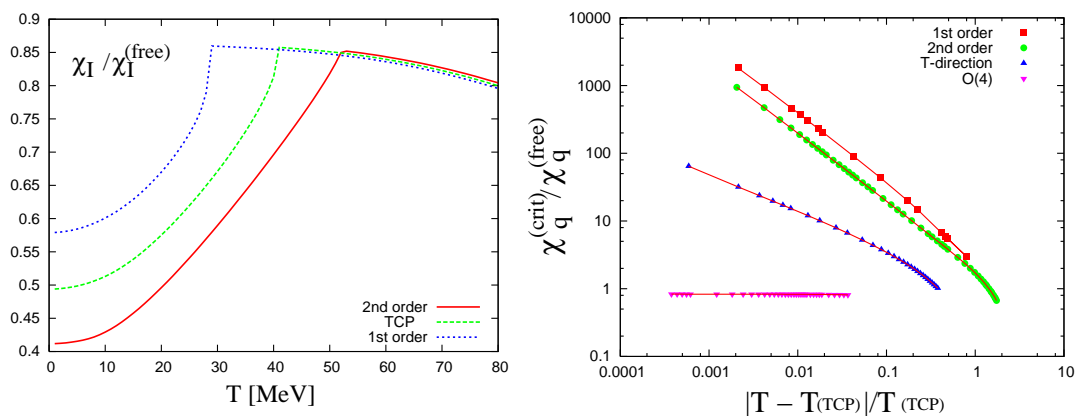


Figure 3. The left-hand figure: the isovector fluctuations versus T for fixed μ_q chosen as in the Fig. 2. The right-hand figure: the quark number susceptibility χ_q near TCP versus $t = |T - T_c| / T_c$ when approaching the TCP along the line of the 1st and the 2nd order transition as well as at constant T . Also shown is χ_q when crossing the O(4) critical line at fixed μ_q [9].

[9, 18, 19]. Fig. 2-right shows the T -dependence of the net quark number susceptibilities in the vicinity and at the TCP. The χ_q varies rapidly with T and drops discontinuously at the phase boundary. The size of this discontinuity grows with increasing μ_q up to the TCP where the susceptibility diverges. Beyond the TCP the discontinuity is again finite. At $\mu_q = 0$ the discontinuity vanishes and the susceptibility shows a weaker, non-analytic structure at the transition temperature. Also at finite quark mass the discontinuity along the cross-over line and at the critical end point is replaced by a peak which diverges at the critical end point. The critical properties of χ_q at the TCP and along the 2nd order line are universal and are governed by different critical exponents.

Fig. 3-right illustrates the critical behavior of χ_q near the 2nd order critical line

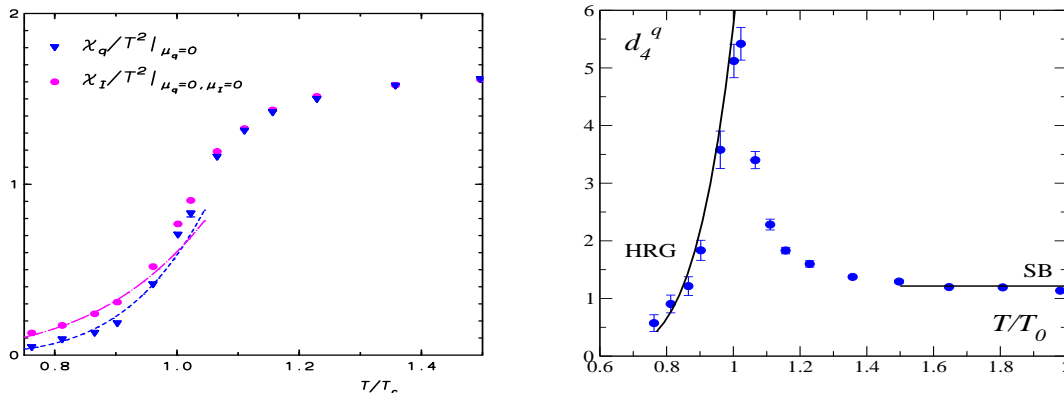


Figure 4. The left-hand figure: the isovector χ_I and the quark number χ_q susceptibilities at $\mu_q = 0$. The right-hand figure: the fourth-order cumulant moments. The results are from LGT calculations with $N_f = 2$ and $m_q \simeq 80$ MeV [14, 17]. The lines for $T/T_0 < 1$ are the hadron resonance gas model results.

and at the TCP. In the mean field approximation the critical dependence of χ_q on the reduced temperature $t = |T - T_c|/T_c$ is consistent with that obtained in the Landau theory [7, 9]. For paths approaching the TCP asymptotically tangential to the phase boundary, the susceptibility diverges with the correlation length critical exponent $\gamma_q = 1$. For other paths the critical exponent is $\gamma_q = 1/2$. Along the second order critical line, the susceptibility remains finite. Going beyond the mean field and including quantum fluctuations in the lagrangian the above critical exponents are renormalized to those belonging to the universality class of the 3D Ising model [18]. On the other hand, the finite value of χ_q along the 2nd order line is consistent with the O(4) universality class [9, 17, 18, 19]. There, the critical properties of χ_q are governed by the specific heat critical exponents $\alpha \simeq -0.2$ [7, 17].[‡] Consequently, at $\mu_q = 0$ the T -dependence of χ_q is only due to the regular part of the free energy [7, 17]. At finite μ_q the singular contribution to χ_q results in the cusp structure the strength of which increases with μ_q . The fourth-order cumulant $d_4^q \simeq \partial^4 P / \partial \mu_q^4$ develops a cusp already at $\mu_q = 0$ and diverges at finite μ_q along the O(4)-line [17].

Contrary to χ_q , the isovector fluctuations χ_I shown in Fig. 3-left are neither singular nor discontinuous at the chiral phase transition. The non-singular behavior of χ_I at the TCP is consistent with the observation that there is no mixing between isovector excitations and the isoscalar sigma field due to the $SU(2)_V$ isospin symmetry[19].

Recently, the net quark as well as isovector fluctuations and higher moments were computed [14, 17] in two flavor lattice QCD (see Figs. 4 and 5). At $\mu_q = 0$, χ_q shows a strong suppression of the fluctuations in confined phase and a cusp-like structure that increases with μ_q in the vicinity of the transition temperature at $\mu_q \neq 0$. Also observed on the lattice was a cusp in the forth-order cumulant moment at $\mu_q = 0$. The lattice

[‡] In the NJL model we obtain the mean-field value for this critical exponent, $\alpha = 0$.

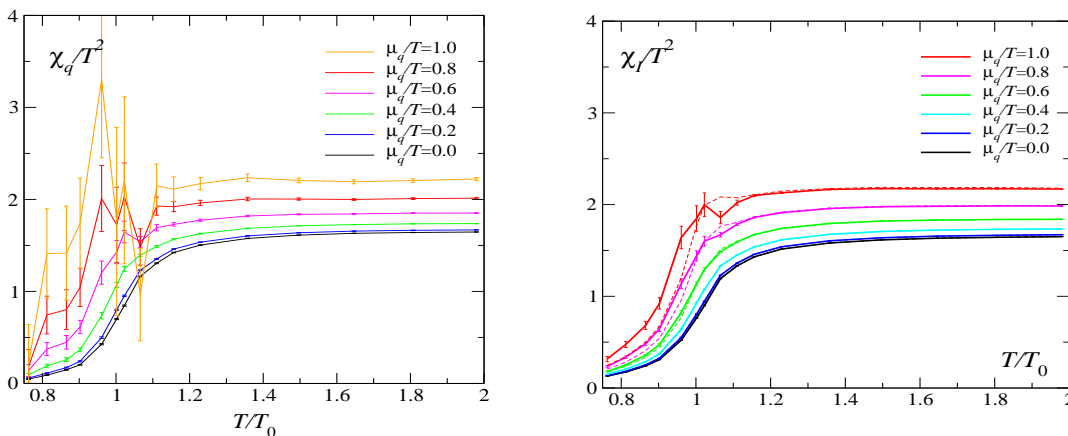


Figure 5. The net quark number χ_q (left-hand figure) and isovector χ_I (right-hand figure) susceptibilities for different values of μ_q/T . The results are from LGT calculations with $N_f = 2$ and $m_q \simeq 80$ MeV [14].

results confirmed that the quark fluctuations in the isovector channel χ_I , contrary to χ_q , do not show any peak structure and depend only weakly on μ_q . These properties of χ_q and χ_I are consistent with O(4) universality arguments and should be there when approaching the critical end point with increasing μ_q . However, the above behavior of χ_q and χ_I can be also interpreted in terms of the regular part of the free energy due to the enhanced contribution of resonances in the vicinity of the transition temperature. The LGT results on T and μ_q dependence of χ_q and χ_I as well as d_q^4 can in the confined phase be successfully described [17] by the resonance gas partition function as seen in Figs. 4. This is also illustrated in Fig. 6, where the ratio $R_{4,2}^q = d_4^q/d_2^q$ of the fourth- to the second-order cumulants as well as the ratio of the quark density to the susceptibility are seen to be consistent with the hadron resonance gas model. The observed change in cumulants at T_c is due to deconfinement resulting in a change of the quark content of particles in a medium. Consequently, the properties of the charge fluctuations seen in Figs. 4-6 are only necessary but not sufficient conditions to verify the existence of a critical endpoint (CEP) in the phase diagram. To verify the existence of the CEP one would need to observe a non-monotonic behavior of the net quark number (or electric charge) susceptibilities as shown in Fig. 7. The non-monotonic behavior of χ_q along the boundary line appears since the quark number fluctuations are finite along the 2nd and the 1st order transition and diverge at the TCP.

The finite structure of the charge susceptibilities along the first order line is valid under the assumption that this transition appears in equilibrium. Admitting deviations from the idealized equilibrium situation, the first order phase transition is intimately linked with the existence of a convex anomaly in thermodynamic pressure [20]. There is an interval of energy or baryon number density where the derivative of pressure $\partial P/\partial V > 0$. Such an anomalous behavior describes the region of instabilities bounded by the spinodal lines where the pressure derivatives taken at constant temperature or

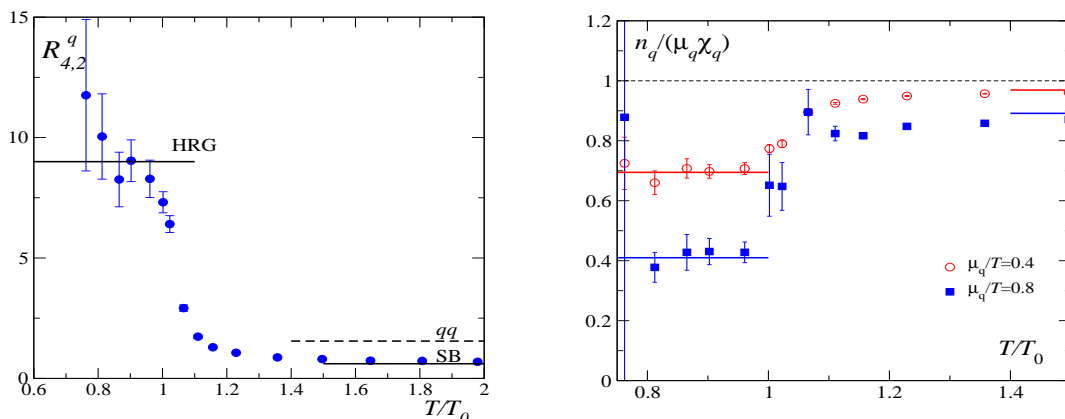


Figure 6. The ratio of fourth- to second-order cumulants of quark number at $\mu_q = 0$ (left-hand figure). The quark number density n_q with respect to the net quark number fluctuations χ_q (right) as a function of T/T_0 for various μ_q/T . Horizontal lines show the infinite temperature ideal gas values and the HRG model prediction (solid lines). The LGT results are from [14, 17]

entropy vanishes. Changing the temperature or entropy results as the isothermal or isentropic spinodal line in the (T, n_q) -plane with n_q being the net quark number density. The spinodal decomposition of the system was argued to enhance the baryon number and strangeness fluctuations [20].

Fig. 8-left shows the phase diagram obtained in the NJL model formulated at finite current quark mass that accounts for spinodal instability. From this figure it is clear that the isothermal spinodal lines end up at the CEP. It is thus natural to explore how the charge fluctuations develop when going beyond the critical end point in the direction of the first order phase transition. Fig. 8-right shows the evolution of the net quark number fluctuations along the path of fixed $T = 50$ MeV in the (T, n_q) -plane. The resulting behavior is quite interesting. When entering the mixed phase there is singularity in χ_q that appears when crossing the isothermal spinodal lines, where the fluctuations diverge and change the sign. Between the spinodal lines the susceptibility is negative. This implies a strong instability in the baryon number fluctuations when crossing the transition region between chirally symmetric and broken phase.

The behavior of χ_q seen in Fig. 8 is a direct consequence of the following thermodynamic relation

$$\left(\frac{\partial P}{\partial V}\right)_T = -\frac{n_q^2}{V} \frac{1}{\chi_q}, \quad (1)$$

what connects the pressure derivative with the charge density n_q and the corresponding susceptibility χ_q . Along the isothermal spinodal lines the pressure derivative in (1) vanishes. Thus, for non vanishing density n_q its fluctuations have to diverge to satisfy the relation (1). In addition, since the pressure derivative $\partial P/\partial V|_T$ changes sign when crossing the spinodal points, there should be discontinuity and the corresponding sign change in the divergence of χ_q as seen in Fig. 8. Due to linear relation between χ_q ,

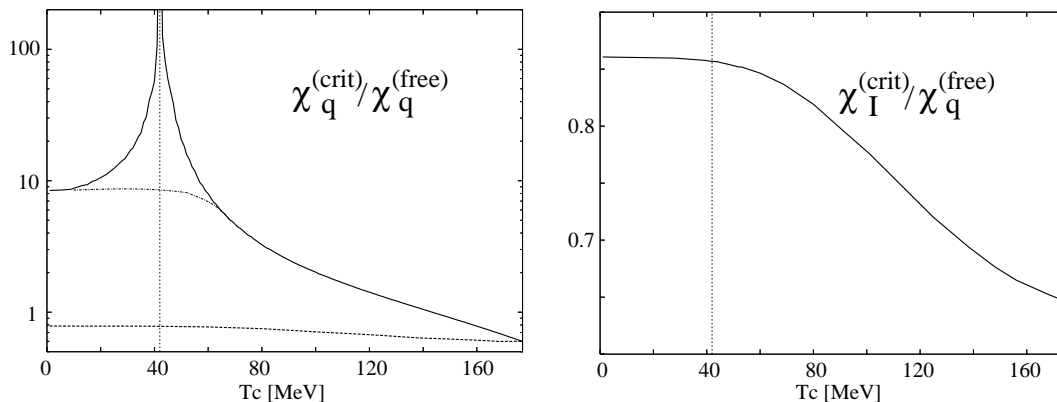


Figure 7. The quark number (left) and isovector (right) susceptibilities χ_q and χ_I as functions of the temperature along the phase boundary. In the left-hand figure the solid (dashed) line denotes χ_q in the chirally broken (symmetric) phase. The vertical dotted-line indicates the position of the tricritical point TCP. The calculations were done in the chiral limit in the NJL model [9].

χ_I and the electric charge susceptibility χ_Q a similar behavior as seen in Fig. 8 for χ_q should be also there for χ_Q .

From Fig. 8 it is clear that when approaching the CEP from the side of the first order transition the region of instability shrinks and disappears completely at the CEP. Consequently, the CEP singularity in χ_q appears from the matching of the two positive singular branches of χ_q . Thus, the singular properties at the CEP are the remnant of divergent behavior of χ_q at the first order chiral phase transition. From the above discussion it is clear that divergent charge fluctuations are not only attributed to the second order critical end point or TCP but are also there at the first order transition if the spinodal phase decomposition sets in. Consequently, the fluctuations of the conserved charges could be considered as a signal of the first order transition that is expected in the QCD phase diagram [21].

In summary, we have presented a brief discussion of the phase structure expected in two flavor QCD. We have discussed the properties of charge density fluctuations when crossing the phase boundary. It was shown that for equilibrium transition the fluctuations of the net baryon number and electric charge exhibit a non-monotonic behavior along the QCD phase boundary that could be applied in heavy ion collisions as the signal for the existence of the critical end point. We have also argued that admitting deviations from the equilibrium picture for the first order transition the above non-monotonic structure is to be modified. In the presence of spinodal instabilities the fluctuations of the conserved charges diverge when crossing the isothermal spinodal lines of the 1st order transition. Consequently, such fluctuations can be used to probe the first order phase transition in heavy ion collisions.

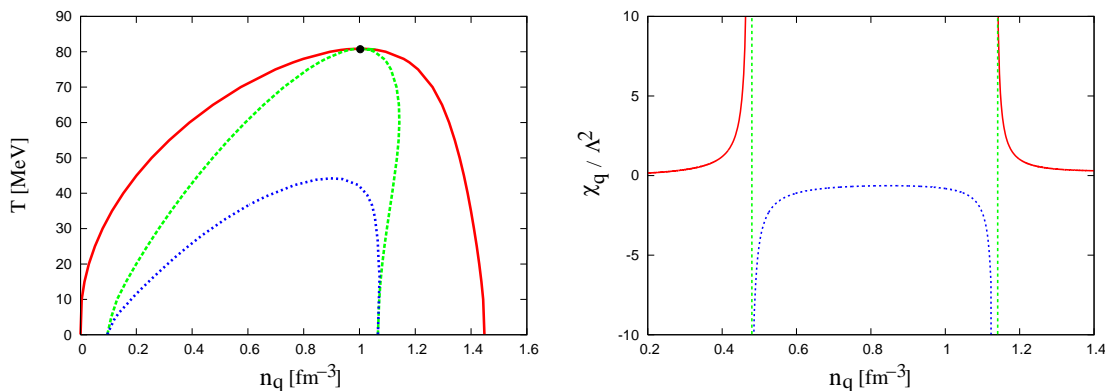


Figure 8. The left-hand figure: The phase diagram in the temperature T and quark number density n_q plane in the NJL model. The filled point indicates the CEP. The full lines starting at the CEP represent boundary of the mixed phase in equilibrium. The broken-curves are the isothermal whereas the dashed-broken ones are the isentropic spinodal lines. The right-hand figure: the net quark number density fluctuations χ_q/Λ^2 normalized to momentum cut-off Λ as a function of the quark number density n_q across the first order phase transition. The χ_q was calculated in the NJL model along the line of constant temperature $T = 50$ MeV.

K.R. acknowledges fruitful collaboration and discussions with S. Ejiri and F. Karsch and the support of the Polish Ministry of National Education (MEN).

- [1] M. Stephanov, Int. J. Mod. Phys. A **20**, 4387 (2005).
- [2] M. A. Stephanov, Phys. Rev. Lett. **76**, 4472 (1996); Nucl. Phys. Proc. Suppl. **53**, 469 (1997)
- [3] M. G. Alford, K. Rajagopal and F. Wilczek, Phys. Lett. B **422**, 247 (1998)
- [4] R. Rapp, T. Schafer, E. V. Shuryak and M. Velkovsky, Phys. Rev. Lett. **81**, 53 (1998)
- [5] J. Berges and K. Rajagopal, Nucl. Phys. B **538**, 215 (1999)
- [6] S. P. Klevansky, Rev. Mod. Phys. **64** (1992) 649. M. Buballa, Phys. Rept. **407**, 205 (2005).
- [7] Y. Hatta and T. Ikeda, Phys. Rev. D **67**, 014028 (2003).
- [8] H. Fujii, Phys. Rev. D **67**, 094018 (2003). H. Fujii and M. Ohtani, Phys. Rev. D **70**, 014016 (2004).
- [9] C. Sasaki, B. Friman and K. Redlich, J. Phys. G **32**, S283 (2006); hep-ph/0609211; hep-ph/0611147.
- [10] C. Ratti, M. A. Thaler and W. Weise, Phys. Rev. D **73**, 014019 (2006)
- [11] R. D. Pisarski and F. Wilczek, Phys. Rev. D **29**, 338 (1984).
- [12] M. A. Halasz et al., Phys. Rev. D **58**, 096007 (1998).
- [13] M. A. Stephanov, K. Rajagopal and E. V. Shuryak, Phys. Rev. Lett. **81**, 4816 (1998).
- [14] C. R. Allton et al., Phys. Rev. D **66**, 074507 (2002); Phys. Rev. D **71**, 054508 (2005).
- [15] R.V. Gavai and S. Gupta, Phys. Rev. D **71**, 114014 (2005).
- [16] Z. Fodor and S. D. Katz, JHEP **0203**, 014 (2002); JHEP **0404**, 050 (2004).
- [17] S. Ejiri, F. Karsch and K. Redlich, Phys. Lett. B **633**, 275 (2006)
- [18] B.-J. Schaefer and J. Wambach, hep-ph/0603256.
- [19] Y. Hatta and M.A. Stephanov, Phys. Rev. Lett. **91**, 102003 (2003)
- [20] P. Chomaz, M. Colonna and J. Randrup, Phys. Rept. **389**, 263 (2004). D. Bower and S. Gavin, J. Heavy Ion Physics **15**, 269 (2002). V. Koch et al., Phys. Rev. C **72**, 064903 (2005).
- [21] C. Sasaki, B. Friman and K. Redlich, arXiv:hep-ph/0702254.